AN INFORMATION THEORETICAL APPROACH TO FUNCTIONAL CONNECTIVITY IN BRAIN

by

Emrah Budur

B.S., in Computer Engineering, Yıldız Technical University, 2007

Submitted to the Institute for Graduate Studies in
Science and Engineering in partial fulfillment of
the requirements for the degree of
Master of Science

Graduate Program in Computer Engineering Department

Boğaziçi University

2011

ACKNOWLEDGEMENTS

It is a wonderful feeling to complete a thesis after a long period of collaborative research. Let me take this opportunity to express my gratitudes for those invaluable people who spared no effort to achieve outstanding results to be published at international level journals. The completion of this work is not only a present for them but also a kind of respect for their precious efforts.

First and foremost, I need to say that formal thanks are inadequate to express my gratitude to my beloved fiancé Oya ÇİMEN who is always a powerful source of energy for me with her existence and consistent support to keep me on the right track.

I offer my sincerest gratitude to my thesis supervisor Dr. Haluk BİNGÖL who is fairly an impeccable master of wisdom. He has willingly sacrified his valueable time to support me with his academic guidance, knowledge and patience whilst giving me the freedom to accomodate my personal priorities. I am most indebted to Dr. Ata AKIN who has generously introduced this groundbreaking topic to me. His expertise and broad vision always accompanied his target-oriented guidance and steadfast encouragement to overcome the odds. It is a golden opportunity for me to meet his true-blue personality.

I owe a duty of good faith and fidelity towards my employer Garanti Technology since attending the university would not be possible unless it was allowed by the company regulation. I owe special thanks to my executive managers Tuba ÇERMİS UZUN, Reha DİRİ and Gürkan SEL who provided me with the freedom to keep balance between studying and working. It is a pleasure also to thank my dear coworkers particularly Muhammed Zahit ÖZDEMİRCAN and Hakan GÜLAP since I was previledged to have generous support and insightful comments from them.

I would like to thank Drs Bedriye ÖNCÜ and Özgür ÖNER for sharing their pa-

tients' data with me and Nermin TOPALOĞLU, Ercan KARA and Burcu ERDOĞAN for collecting the fNIRS data

Above all, my chief thanks ever remain to God, The Merciful, for granting me the chance to collaborate with the network of excelent people to complete this thesis.

ABSTRACT

AN INFORMATION THEORETICAL APPROACH TO FUNCTIONAL CONNECTIVITY IN BRAIN

Mental disorders are usually associated with functional abnormalities of brain that are revealed by behavioral symptoms. Attention-deficit hyperactivity disorder (ADHD), in particular, is well known to be a common behavioral disorder with characteristic symptoms of inattentiveness, impulsivity and hyperactivity which impairs the life quality of the individuals. Although the characteristics of ADHD is well defined, the neurobiological reasons of this disorder is not fully discovered yet. The introduction of functional near infrared spectrocopy (fNIRS), which is a novel non-invasive optical imaging technology, provided an easy way to reveal hemodynamics of ADHD in brain.

In this study, our aim was to find an information theoretical method to diagnose adults with ADHD via fNIRS. We assigned 10 ADHD subjects to experimental group and 12 control subjects to the control group. Each subject in experimental group is involved in two experimental runs which are executed when they are with and without medication denoted by ADHD-ON, ADHD-OFF, respectively. On the other hand, a single experimental run, which is denoted by CONT, is performed for the control group. The subjects performed the Stroop test in experiments.

One-way ANOVA analysis was conducted among three groups of data, namely ADHD-OFF, ADHD-ON and CONTROL, to compare the effect of MPH. Given the significance level of $\alpha = 0.05$, the result $F = 6.86, p = 0.0036$ indicates that the values of three groups differ significantly from each other.

As a result, it is observed that medication normalizes the brain signals of the

individuals in ADHD group towards healthy controls.

Keywords: ADHD, fNIRS, Functional Connectivity, Mutual Information.

ÖZET

BEYİNDEKİ İŞLEVSEL BAĞLILIĞA BİLGİ TEORİSİ YAKLAŞIMI

Zihinsel hastalıklar, davranışsal belirtiler ile anlaşılmakta ve genellikle beyindeki işlevsel bozuklukların sonucu olarak ortaya çıkmaktadır. Özellikle Dikkat Eksikliği Hiperaktivite Bozukluğu (DEHB), sık görülen bir davranışsal hastalık olup dalgınlık, ataklık, aşırı hareketlilik gibi belirtiler ile kendini göstermekte ve hastanın yaşam kalitesini düşürmektedir. ADHD'nin temel belirtileri çok iyi tanımlanmış olmasına rağmen bu hastalığın nörobiyolojik sebepleri henüz tam olarak belirlenememiştir. Diğer yandan, oldukça yeni ve noninvazif bir görüntüleme teknolojisi olan işlevsel yakın kızıl ötesi spektroskopi (İYKS) yönteminin günümüzde kullanılmaya başlaması, DEHB'nin beyindeki etkilerinin çok kolay bir şekilde ortaya çıkarılmasını sağlamıştır.

Bu çalışmadaki amacımız, bilgi teorisinden faydalanarak, İYKS teknolojisi ile yetişkin DEHB hastalarını teşhis edebilecek bir yöntem geliştirmektir. Bu kapsamda 10 DEHB hastası ve 12 sağlıklı birey üzerinde deney yapılmıştır. Deney grubundaki her denek, ilaç almadan önce ve ilaç aldıktan sonra olmak üzere ikişer deneye tabi tutulmuştur. Diğer yandan kontrol grubundaki denekler birer deneye tabi tutulmuştur. Elde edilen veri gruplarına sırasıyla ADHD-OFF, ADHD-ON ve CONT olarak isimlendirilmiştir. Deneylerde deneklere Stroop testi uygulanmıştır.

MPH isimli ilacın DEHB hastaları uzerinde etkisini incelemek üzere üç veri grubu arasında tek yönlu ANOVA analizi yapılmıştır. Hassasiyet değeri olarak $\alpha = 0.05$ belirlenmiştir. Analiz sonucunda elde edilen değerler ($F = 6.86, p = 0.0036$) üç veri grubu arasında istatistiksel olarak anlamlı bir farklılık olduğunu ortaya koymuştur.

Sonuç olarak, ilaç tedavisinin, hasta bireylerin beyin sinyallerini, sağlıklı bireylerinkine benzer şekilde normalleştirdiği gözlemlenmiştir.

Anahtar sözcükler: DEHB, İYKB, İşlevsel Bağlılık, Ortak Bilgi.

TABLE OF CONTENTS

LIST OF FIGURES

LIST OF TABLES

LIST OF SYMBOLS

F	Test of statistics
α	Significance Level
σ	Standard Deviation

LIST OF ACRONYMS/ABBREVIATIONS

ANOVA	Analysis of Variance
ADHD	Attention-Deficit Hyperactivity Disorder
CBF	Cerebral Blood Flow
df	Degree of freedom
DSM	Diagnostic and Statistical Manual of Mental Disorders
DSM-IV	The fourth revision of DSM
DSM-IV-TR	A ”Text Revision” of DSM-IV
EEG	Electroencephalogram
fMRI	Functional Magnetic Resonance Imaging
fNIRS	Functional Near Infrared Spectroscopy
MSE	Mean Square for Error
MSTr	Mean Square for Treatment
NIRS	Near Infrared Spectroscopy
SCID	Structural Clinical Interview for DSM-IV-TR AXIS I Disorders

1. INTRODUCTION

Functional neuroimaging is the field of study in which multitude of brain imaging modalities are employed to investgate the neurobiological and anatomic changes occurring during health and disease. *Functional near infrared spectrocopy (fNIRS)*, has shown promise among these modalities as a non-invasive, accurate, rapid and comfortable technique that also posseses high sensitivity and specifity to cortical hemodynamics, specifically the frontal lobe.

Attention-deficit hyperactivity disorder (ADHD) is a common pediatric disorder persisting across adolescence and adulthood with characteristic symptoms of impulsivity, lack of attention and hyperactivity [1]. Although these core symptoms have been known to clinicians since the late 19th century, the methods used to diagnose ADHD revolutionalized dramatically. Studies with noninvasive structural and functional neuroimaging techniques, i.e. MRI, identified significant abnormalities in frontal regions of brain in ADHD patients [2–5]. A growing body of converging data of ADHD patients implies decrease in frontal brain circuitry which is already known to be responsible for attentional, cognitive and executive function [6].

The functional imaging techniques provided unparalelled ways to discover the pathophysiology of ADHD and the biological effects of medications [6]. An increasing number of influential research papers were published to investigate a variety of psychiatric diseases via fNIRS [7–10]. Finally, analysis of ADHD via fNIRS began to make an overwhelming impression on neuroscientists [11–13]. Studies performed with fMRI & fNIRS mainly focused on "where" and "how much". Recent discoveries in neuroscience showed that the brain prefers to operate in a "connected" way and share information to address a stimulus. New metrics of brain connectivity were immediately employed by fMRI and fNIRS researchers [14–16] to investigate the functional connectivity of the brain while subjects were engaged with a cognitive tasks.

Application of information theory to fMRI analysis has well-known to be successfull to reveal brain connectivity, for the last decade [17–20]. To the best of our knowledge, fNIRS device has not yet been employed with an information theoretical approach to investigate ADHD subjects. Therefore, this thesis attempts to address the need to find an information theoretical method to investigate adults with ADHD via functional connectivity of fNIRS signals. The main hypothesis we wish to address is "ADHD manifests itself as a loss of connectivity in the prefrontal cortex but it normalizes with medication".

2. BACKGROUND

This study required a background on multidisciplinary areas including psychiatry, neuroimaging, signal processing, information theory and statistics. Below are brief explanations of the essential subjects that are meant to provide a firm foundation for the rest of the chapters.

2.1. History of Mental Disorders

According to most historians, mental disorder was thought to be abnormal behaviours which were seen as a victory of evil spirits over good spirit on human body. Archaeological excavations help discover skulls with holes. Historian claims that these skulls were cut away by a stone instrument to let the evil spirit leave the body. This process, which is called trepanning, was replaced by a non-invasive method of priests, namely exorcism [21].

The introduction of scientific approach to address abnormal behaviours dates back to 1790s. The idea was pioneered by French physician Philippe Pinel who was also known as a founder of modern psychiatry [22]. He suggested that mentally ill people deserve to take medical treatment and could be treated by identifying both psychological and physiological factors [23].

The biological model is proposed in late 19th century with the prominent hazardous case of Phineas Gage, who is known as a survival of the accident in which a bar stick was projected from his chin, out of the top of his head. He was surprisingly alive with serious brain damage in his forehead. However, it was soon realized that he turned out to be irreverent, profane and rude to his colleagues [24]. Harlow reported that damage in Cage's brain, destroyed the equilibrium between his intellectual faculties and animal propensities [25]. These studies presented a clear case for a further and deeper investigation of brain dynamics to diagnose and treat mental disorders.

2.2. Attention-Deficit Hyperactivity Disorder

Attention-deficit hyperactivity disorder (ADHD) is an early-onset psychiatric disorder which poses characteristic behavioral symptoms of impulsivity, lack of attention and hyperactivity across adolescence and adulthood. The signs of inattention include daydreaming, distractibility, and difficulty focusing on a single task for a prolonged period. The inattention component is accompanied by the hyperactivity component which is expressed as fidgeting, excessive talking, and restlessness [26].

ADHD is a highly prevalent neurobehavioral disorder that afflicts children, in particular. Related studies found that ADHD affects 8-12% of children worldwide. Half of the ADHD diagnosed children have continuing symptoms persisting into adulthood [27]. In recent years, the pravalence in adults is getting increasingly recognized and society began to suffer from ADHD in terms of financial cost, stress to families and disrupts in academic and vocational goals [26].

The complex etiology and strong genetic underpinnings make ADHD a multifactorial disorder. Although its etiology remains unclear, converging evidences support the hypothesis that the underlying neurobiological factor of the disorder is deficits in the frontal lobe functions and connections between frontal lobe and key subcortical regions. The investigators of latest neuroimaging studies identified common structural and functional brain abnormalities among ADHD patients [26].

2.3. Brain Connectivity

In the recent years, modern science played a key driving force to discover not only the building blocks of brain but also the functional properties of brain. The advancement in technology helped to appreciate the human brain as a complex network of neurons which are responsible for executive functions including decision taking, pursuing long-term goals, controlling thoughts [24]. Recent studies in neuroscience investigated the phenomenon underlying the functional activities of the human brain by scrutinizing neural connections.

Friston suggests that there are different types of connectivity patterns which can be applied to human brain. Anatomical connectivity refers to physiological and structural connections among networks of neurons while functional connectivity is described to be the statistical dependencies between remote neurophysiologic changes. Effective connectivity is, on the other hand, causal relationship between neuronal systems [28]. Brief explanation of each connectivity type is given below.

2.3.1. Anatomical Connectivity

The basic building blocks of brain are neurons. Each neuron is anatomically connected to other neurons to communicate each other with electrochemical reactions through synapses. Consequently, the brain works by forming networks of interconnected neural cells that are specialized to transmit information. Briefly, anatomical connectivity refers to the physical relationship of neuronal units.

2.3.2. Functional Connectivity

Unlike anatomical connectivity, functional connectivity does not imply a direct physical connection. It is, rather, a statistical concept. The concept of functional connectivity is defined by Friston as *the correlations between spatially remote neurophysiological events* [29] which refers to the statistical dependency of the physiological changes across physically seperated neuron populations during experiments.

Introduction of functional connectivity concept has given weight to the long-standing idea that mental ilnesses are direct consequences of the lack of communication among brain regions. The latest studies show that functional connectivity analysis is considered to be the most reliable measurement method for the level of mental diseases such as Alzheimer's disease, epilepsy, ADHD and schizophrenia [30–35].

2.3.3. Effective Connectivity

Similar to functional connectivity, effective connectivity is defined as the statistical relationship between regions of brain. In contrast to functional connectivity, effective connectivity is a causal relationship which is defined as *the influence one neuronal system exerts over another* [29]. Putting it in a nutshell, effective connectivity is considered to be the union of anatomical connectivity and functional connectivity.

2.4. Functional Near Infrared Spectroscopy (fNIRS)

The recent advancements in imaging technologies has offered neuroscientists the golden opportunity to monitor cognitive functions of brain in correspondence with the hemodynamic changes in *cerebral blood flow (CBF)*. It is well-known that a large fraction of energy resource, which is carried by the blood flow as glucose and oxygen, is consumed by the brain [30]. Therefore, at any given time, the CBF to the relevant neuronal units increases to address demand of a particular active brain region. The basic principle of all brain imaging technologies is detecting and mapping these hemodynamic changes in CBF and cerebral metabolism [30].

As one of the emerging brain imaging technologies, near infrared spectroscopy (NIRS) has been shown to provide a non-invasive approach that relies on the fact that oxygenated blood flow reflects different amount of light than deoxygenated blood flow [36]. As a direct consequence, it can be inferred that activated brain regions reflect different amount of light than inactive brain regions. fNIRS is the detection and assessment of the optical changes of CBF associated with the functional activity of the brain [37].

The differential light reflection can be precisely measured with high temporal resolution by means of optical recording devices [30]. Basically, the source of light emits the light through the skull and then the receptors measures the amount of light reflected by the underlying tissues (See Fig.2.1). For a review of fNIRS technology, please refer to the related references [37–39].

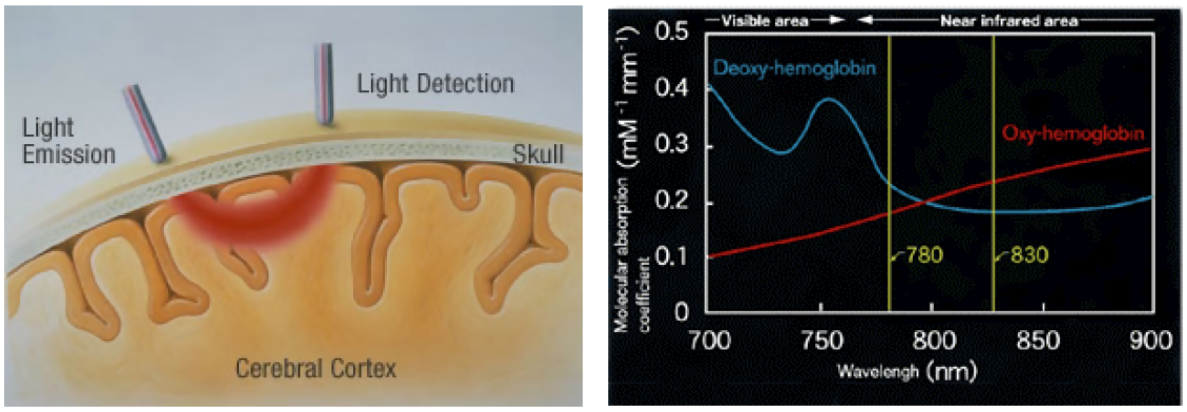

(a) The pathway of light in NIRS

(b) The light absorbtion spectra of oxygenated blood flow

Figure 2.1. Illustration of how NIRS works [37].

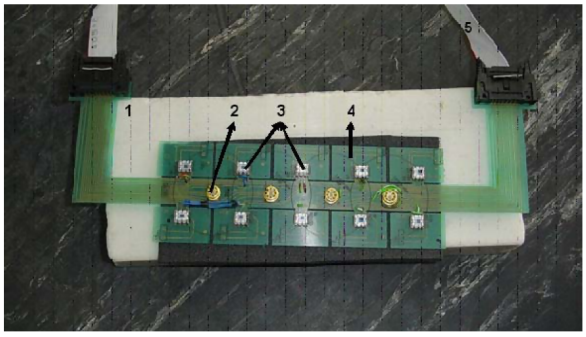

Figure 2.2. NIROXCOPE 301 device components. (1) A Gray phantom. (2) 4-LED probe. (3) 10 photodetectors. (4) PCB. Adopted from [39].

The device that is used in this study is called NIROXCOPE 301 which was built in Biophotonics Laboratory of Bogazici University [40–42]. It is a novel device developed specifically for fNIRS studies. It has 4 sources of light along with 10 surrounding light receptors (See Fig.2.2). At any moment, only a single light source emits light while the surrounding 4 receptors are detecting and recording the amount of reflected light. In this way, the crosstalk between adjacent brain regions is minimized.

2.5. Mutual Information

There are a number of different types of methods to calculate statistical dependency of neural activities, for instance mutual information analysis, one of the basic

measurement methods of Shannon's Information Theory [43]. In contrast to other types of metrics such as correlation and coherence, mutual information is appropriate choice of metric since it is a metric for also determining nonlinear statistical dependencies of neural signals [44, 45]. In addition, coherence function might be zero even if the variables are related to each other as examplified in [46]. In contrast to coherence function, the output of mutual information is consistent and zero if and only if the signals are statistically independent [46]. Therefore, mutual information is chosen as the dependency function.

There are a couple of different approaches to calculate mutual information. The classical one is based on entropy and originated by Shannon [43]. On the other hand, it can also be calculated based on coherence in frequency domain [14, 46, 47]. The calculation of mutual information in this study is based on the method suggested by [47].

Salvador et al. presented a method to calculate mutual information of time-series (i, j) in frequency domain [14]. Zhou et al. modified and represented it as follows [44] :

$$\delta_{ij} = \frac{1}{2\pi}\int_{\lambda 1}^{\lambda 2} \log(1 - coh_{ij}(\lambda))\, \mathrm{d}\lambda \tag{2.1}$$

where the cross coherence function $coh_{ij}(\lambda)$ is given as

$$coh_{ij}(\lambda) = |R_{ij}(\lambda)|^2 = \frac{|f_{ij}(\lambda)|^2}{f_{ii}(\lambda) f_{jj}(\lambda)} \tag{2.2}$$

where $f_{ij}(\lambda)$ is the cross spectral density between time-series (i, j); $f_{ii}(\lambda)$ and $f_{jj}(\lambda)$ are spectral densities of ith and jth time-series respectively [44].

2.6. Test of Hypothesis

2.6.1. Student's *t*-test

Student's *t*-test is one of the most commonly used statistical hypothesis test. It is introduced by the British statistician William Sealy Gosset who published his influential paper under the pseudonym *Student* [48, 49]. It provides a method to identify whether the variance of the difference between the two related set of data is statistically significant. Student's *t*-test statistics can be used when

- to test null-hypothesis that the population mean is likely to be equals to the hypothesized value;
- to detect the difference between measurements collected from two different groups of population;
- to estimate if there is a significant difference between the means of two measurements collected from the same group, before and after an intervention in an experimental study.

There are three types of *t*-test calculation such as one-sample *t*-test, independent sample *t*-test and paired *t*-test. Although all types of *t*-test are similar in calculation, the procedural overview of performing each type of *t*-test differs. The types of *t*-test will be examined in the subsequent sections. For further details the related references can be referred [50–53].

All types of *t*-test involves calculation of a *t*-score which is of the form given in equation (2.3) [51].

$$t\text{-score} = \frac{\text{estimate - parameter}}{\text{standard error of the estimate}} \tag{2.3}$$

Briefly, *t*-test statistics is a method to measure the distance between the estimated value and the parameter [51]. Fig. 2.3 shows the flow of the general procedure

that is used in all types of t-test applications.

1. State the null hypothesis H_0 and the alternative hypothesis H_1. After completing the following series of steps, either H_0 or H_1 will be accepted.
2. Calculate the t-score based on equation (2.3). The denominator varies depending on the type of t-test applied. Hence, each type of t-test has its own formula to calculate t-score.
3. Calculate *degree of freedom (df)* which depends on the type of t-test. The formula of the degree of freedom is given under the section of each type of t-test application.
4. Given α as the the significance level, find the critical value $t_{\alpha,df}$ from the table of t-distrubution.
5. Compare calculated t-score and $t_{\alpha,df}$. If t-score $< t_{\alpha,df}$, then the null hypothesis H_0 is accepted.

Figure 2.3. General procedure of t-test applications

One-sample t-test

One-sample t-test provides a method to test if the population mean is equal to the hypothesized value. One-sample t-test let the experimenter test if his hypothesized value for the mean is likely or unlikely to be true by comparing the average of a randomly selected sample set against the hypothesized value. If the final outcome of t-test calculation is in acceptance range, the hypothesis is accepted.

The equation t-score of one-sample t-test calculation is given as follows:

$$t\text{-score} = \frac{\overline{X} - \mu_0}{\frac{s}{\sqrt{n}}} \tag{2.4}$$

where $\overline{X}$ is the mean of sample set, μ_0 is the hypothesized value, s is the standard deviation of the sample set and n is the size of the sample set [54]. The degree of

freedom for one-sample t-test application is calculated as $df = n - 1$ [54].

2.6.1.1. Independent samples t-test. Independent samples t-test is used when two groups of samples are not connected to each other in any way. It helps the experimenter compare the mean of measurements of two unrelated groups. For example, the experimenter may wish to figure out if there is a significant difference between the total amount of monthly expenditure of men and women.

The equation t-score of independent t-test calculation is given as follows:

$$t\text{-score} = \frac{\overline{X}_1 - \overline{X}_2}{\sqrt{\left(\frac{n_1 {s_1}^2 + n_2 {s_2}^2}{n_1 + n_2 - 2}\right)\left(\frac{n_1 + n_2}{n_1 n_2}\right)}} \tag{2.5}$$

where $\overline{X}_i$ is the mean, s_i is the standard deviation, n_i is the size of the sample set where $i \in \{1, 2\}$ [54]. The degree of freedom for independent t-test application is calculated as $df = n_1 + n_2 - 2$ [54].

2.6.1.2. Paired t-test. In paired t-test calculation, unlike the independent samples t-test, the measurements are collected from the same participant at different times or from different sites. The paired t-test compares the measurements within participants, in other words the measurement of a participant collected at an earlier status is compared with the measurement of the same participant collected at later status [52]. Therefore, what is important in paired t-test method is not the variation between different participants but variation between pairs of measurements [50]. In this sense paired t-test method suit best for detecting treatment differences or treatment efficency.

The equation t-score of paired t-test calculation is given as follows:

$$t\text{-score} = \frac{\overline{X} - \overline{Y}}{\frac{s_D}{\sqrt{n}}} \tag{2.6}$$

where $\overline{X}$ and $\overline{Y}$ are the first and second observations, respectively, D is the difference between the first and second observation within a pair, s_D is the standard deviation of the differences D and n is the number of observations [54]. The degree of freedom for independent t-test application is calculated as $df = n - 1$ [54].

2.6.2. Analysis of Variance

Broadly speaking, *the analysis of variance (ANOVA)*, refers to the statistical procedure to estimate the variation within the sets of experimental data. The main difference of ANOVA from t-test is that ANOVA can be applied also to more than two datasets.

In the scope of this study, *one-way ANOVA*, which is the most common and simplest type of ANOVA, is implemented. Basically, it involves analysis whether there is a significant difference within means of three or more particular datasets that are categorized by only one factor [54]. For instance, in this study, the effect of medication is the key factor that differentiates the measurements taken from the subjects.

Once one-way ANOVA is decided to be applied, the next step is to state the null hypothesis H_0. H_0 is usually stated as *the means of the experimental data sets are identical*. In other words, all samples are drawn from populations that have identical mean value. On the other hand, the alternate hypothesis H_1 is stated as *at least one of the experimental data sets have different mean value from the rest of the experimental data sets*.

The application of one-way ANOVA test follows calculation of the following series of formulas such as *the mean square for treatment (MSTr)*, *the mean square for error (MSE)* and *the test statistics F*.

$$MSTr = \frac{J}{I-1}\sum_{i}^{I}\left(\overline{X}_i - \overline{X}\right)^2 \tag{2.7}$$

$$MSE = \frac{1}{I}\sum_{i}^{I} {S_i}^2 \tag{2.8}$$

$$F = \frac{MSTr}{MSE} \tag{2.9}$$

where I is the number of data groups compared, J is the number of observation in each data group, S_i is the variance of the samples in ith data group.

The equations (2.7), (2.8), (2.9) form the anatomy of one-way ANOVA analysis. The accompanying Table 2.1 is the standard tabular way of showing the results of these equations.

Table 2.1. Standard table of ANOVA.

Source of Variation	**df**	**Mean Square**	**f**
Treatment	$I-1$	$MSTr$	$MSTr/MSE$
Error	$I(J-1)$	MSE	
Total	$IJ-1$		

As a final result, the value of F provides evidence for or against the acceptance of the null hypothesis H_0. It can be noted that H_0 is true as long as the means of the groups are identical resulting in small value of $MSTr$. On the other hand, MSE depends only on the variance and not on where the means of various distributions are centered. Consequently, $F > 1$ case corresponds to the inequality $MSTr > MSE$. Thus, $F > 1$ case casts considerable doubt on the validity of H_0. After F is calculated, it is evaluated by the cutoff value c where the rejection region is $F \geqslant c$ and acceptance region is $F < c$. Given the significance level α, which is typically either 0.05 or 0.01, the cut off values are determined by looking up F-Distribution table [54]. To put in a nutshell, when applying one-way ANOVA analysis, H_0 is not rejected as long as the calculated F value is within the acceptance region.

3. METHOD

3.1. Experimental Protocol

3.1.1. Subjects

The experimental group consists of 10 ADHD subjects (Age: 18-34, 4 females, 6 males) which are diagnosed by the standard diagnosis criteria of ADHD, namely *Diagnostic and Statistical Manual of Mental Disorders, Fourth Edition* (DSM-IV) [55]. On the other hand, a group of 12 age and gender matched healthy subjects are enrolled to form the control group.

Structured Clinical Interview for DSM-IV, namely SCID-I [56], is applied to both ADHD subjects and healthy controls in order to investigate their current and lifetime psychological status such as anxiety disorder(social phobia), schizophrenia, major depression, substance dependence (except for smoking) and bipolar affective disorders. The interview revealed that one of the ADHD subjects had current anxiety disorder, three of the ADHD subjects had a lifetime history of major depression. SCID-I showed that healthy controls had no current psychiatric diagnosis. Besides, three of the ADHD subjects were asked to stop taking regular MPH medication at least 48 hours before the assesment. The protocol has been approved by the Ethics Committee of Ankara Yıldırım Beyazıt Training and Research Hospital, formerly known as Dışkapı SSK Hospital.

3.1.2. Neuropsychological Experiments

The subjects performed a revised version of the color-word matching Stroop interference test [57]. The Stroop test is often employed to investigate attention related disorders, ADHD in particular [58, 59]. The proven success of Stroop test to measure the inhibition ability of competing responses made it indispensable technique to investigate attentional disorders. It is even considered to be ”The Gold

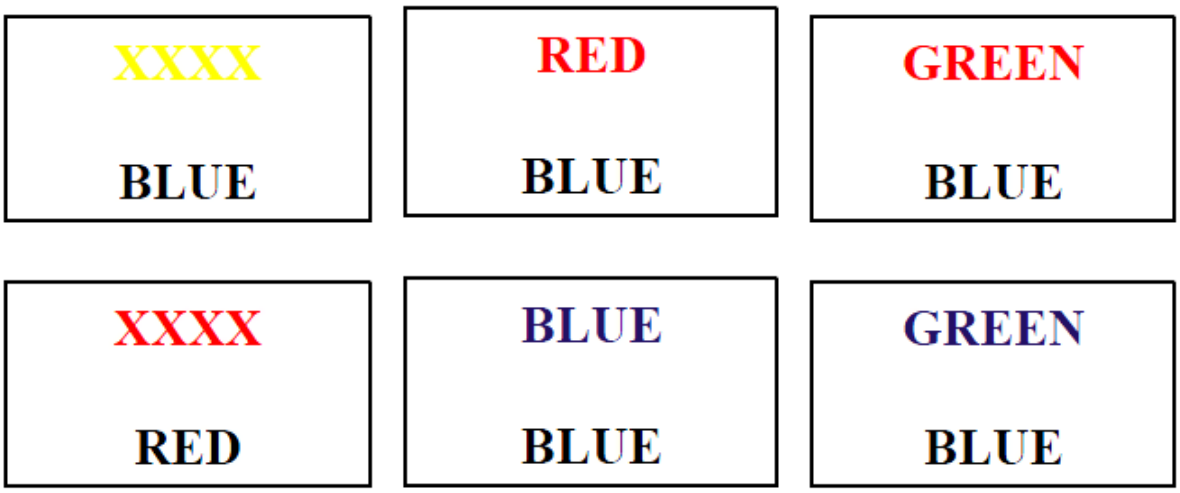

(a) Neutral word-pairs (b) Congruent word-pairs (c) Incongruent word-pairs

Figure 3.1. The examples of word-pairs in Stroop test. The stimuli on the top row are to be marked "wrong" or "unmatched" while the stimuli at the bottom are "correct" or "matched". Adopted from [38].

Standard" of attentional measures [60].

During the Stroop test, subjects were presented a stack of two words as shown in Fig. 3.1 The upper word is ink colored, whereas the lower one is in solid black. The subject was supposed to detect the word-pairs in which the lower word is the color name of the upper word. The meaning of upper word has no importance.

The task involves detecting congruent, incongruent and neutral word-pairs. In *incongruent case*, the color of upper word is conflicting with the lower word (e.g. GREEN the upper word, RED as the lower word). In *congruent case*, on the other hand, the lower word is exactly naming the color of the upper word (e.g. RED as both the upper word and the lower word). In *neutral case*, a nonverbal control stimulus is introduced as the upper word to reduce *interference effect* (e.g. a series of X's in GREEN as upper word, RED or GREEN as lower word) [61].

The subject is asked to detect conflictions in word-pairs and press left mouse with their forefinger in match cases, press right mouse button in with their middle finger in unmatch cases. Stacks of word-pairs are screened in sequence with the

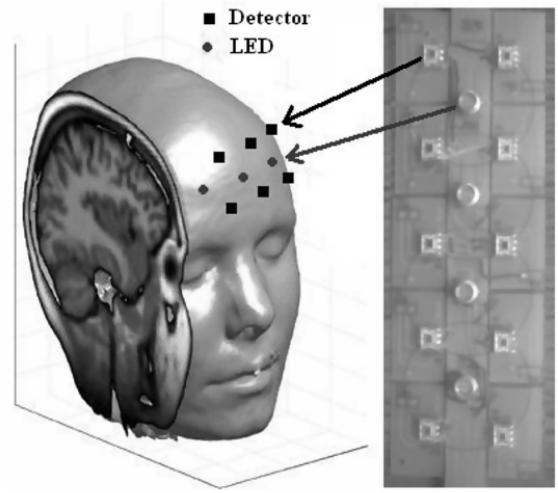

(a) NIROXCOPE 301 alignment [62]

(b) NIROXCOPE 301 in action [64]

Figure 3.2. NIROXCOPE 301 usage.

maximum allowed response time of 2.5 seconds [62]. The interstimulus interval is 4 seconds. Each case is presented in a block containing 6 questions spaced 4 seconds apart. A rest of 20 seconds follows each block.

3.1.3. Data Collection

The datasets published in [39, 63], is used as the data source in this study.

Experiments were carried by using NIROXCOPE 301 aligned on the forehead of the subject as shown in Fig. 3.2a. In order to prevent sweating and external intervention, the experiment were carried in an isolated room with controlled temperature as shown in Fig. 3.2b

In each *experimental run*, the raw data collected from each detector is used to calculate the relative oxygenation change in CBF. The calculation was performed according to modified Beer Lambert Law [42, 62]. Then, the calculated data is preprocessed by applying band pass filter at 0.03-0.25 Hz to eliminate outlier spikes. The band pass filter was implemented by using the ”butter” command in MATLAB. Since NIROXCOPE 301 provides data for 16 channels, the final outcome was series of 16 fNIRS signals which are represented by $\{s_k\}_{k=1}^{16}$. Fig. 3.3 shows a plot of 16

overlayed fNIRS signals recorded from a subject during an experimental run.

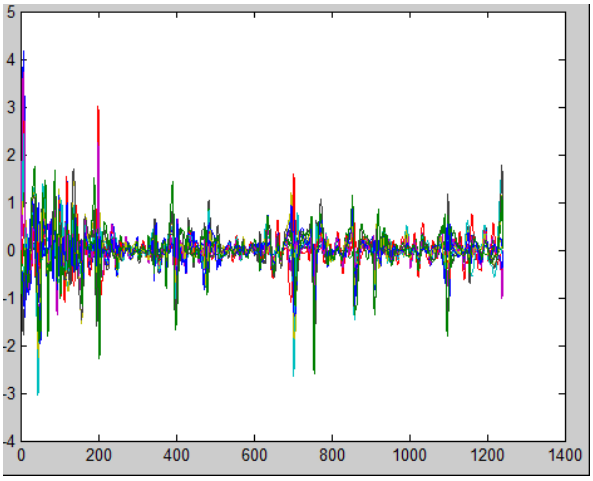

Figure 3.3. The plot of 16 fNIRS signals recorded from a subject during an experimental run.

To sum up, in each experimental run, a group of 16 fNIRS signals are obtained from the subject.

3.2. Data Processing

3.2.1. Mathematical Notation

In this section, the notations that are frequently used in subsequent sections will be explained.

Let X and Y be $n \times m$ real matrices. The ith, jth entry of matrix X is represented as $[X]_{ij}$. *ξ-threshold operator* on matrix X defined as

$$[\tau(X,\xi)]_{ij} = \begin{cases} [X]_{i,j}, & [X]_{i,j} \geqslant \xi, \\ 0, & \text{otherwise.} \end{cases} \tag{3.1}$$

Similarly, the *binary threshold operator* is defined as

$$[\beta(X)]_{ij} = \begin{cases} 1, & [X]_{i,j} > 0, \\ 0, & \text{otherwise.} \end{cases} \tag{3.2}$$

Array multiplication of X and Y is defined as

$$[X \odot Y]_{ij} = X_{ij} Y_{ij}. \tag{3.3}$$

Let M be a binary $n \times m$ matrix, that is $[M]_{ij} \in \{0, 1\}$. Then matrix X *masked* by matrix M would be $X \odot M$.

The *average of nonzero entries* of $X \odot M$ is defined as

$$\lambda(X, M) = \frac{\sum_{i=1}^{n} \sum_{j=1}^{m} [X \odot M]_{ij}}{\sum_{i=1}^{n} \sum_{j=1}^{m} [M]_{ij}} \tag{3.4}$$

Finally, a sequence $X_1, X_2, \ldots, X_p$ of $n \times m$ real matrices is represented by $\{X_k\}_{k=1}^{p}$. The *average* of the sequence is defined as

$$\mu\left(\{X_k\}_{k=1}^{p}\right) = \frac{1}{p} \sum_{k=1}^{p} X_k. \tag{3.5}$$

Note that $\tau(X, \xi)$, $\beta(X)$, $X \odot Y$, and $\mu\left(\{X_k\}_{k=1}^{p}\right)$ are $n \times m$ real matrices. $\lambda(X, M)$ is a real number.

3.2.2. Mutual Information Matrices

Let $\{s_k\}_{k=1}^{16}$ represents the channels of 16 fNIRS signals recorded from a subject, during a single experimental run. Let the signal pair s_i and s_j has the mutual information value that is denoted by $I(s_i, s_j)$. $I(s_i, s_j)$ is calculated by the MATLAB toolbox for functional connectivity given in [44]. Then, the 16×16 *mutual information matrix* of the subject is defined as

$$[X]_{ij} = I(s_i, s_j). \tag{3.6}$$

where $i, j \in \{1, \ldots, 16\}$.

The group of 10 ADHD subjects are assigned to the experimental group and 12 control subjects to the control group. Each subject in experimental group is involved in two experimental runs which are executed when they are with and without medication in a cross-over manner denoted by ADHD-ON, ADHD-OFF, respectively. On the other hand, a single experimental run, which is denoted by CONT, is performed for the control group.

Then, the mutual information matrices of ADHD-OFF, ADHD-ON, and CONT data are denoted as $\{A_k\}_{k=1}^{10}$, $\{B_k\}_{k=1}^{10}$, and $\{C_k\}_{k=1}^{12}$, respectively.

3.2.3. Masking

It is an expected result that the higher values in 16×16 mutual information matrices imply higher mutual information between the corresponding signal pairs. Likewise, the lower values in 16×16 mutual information matrices imply that the corresponding signal pairs are unrelated. A binary *mask matrix* M can be used to eliminate the low values of 16×16 mutual information matrices. The calculation method of M in question will be explained shortly.

The masking operator $\odot$ is used to eliminate the low values. For instance, the

sequence of 10 ADHD- mutual information matrices $\{A_k\}_{k=1}^{10}$, can be masked by M to obtain a masked sequence $\{A_k \odot M\}_{k=1}^{10}$. By applying the average of nonzero entries operator λ, a sequence of 10 real numbers, $\{a_k\}_{k=1}^{10} = \{\lambda(A_k, M)\}_{k=1}^{10}$, is obtained.

As for the ADHD-ON case, similar process is performed to obtain another sequence of 10 real numbers, $\{b_k\}_{k=1}^{10} = \{\lambda(B_k, M)\}_{k=1}^{10}$. Finally, a sequence of 12 real numbers, $\{c_k\}_{k=1}^{10} = \{\lambda(C_k, M)\}_{k=1}^{12}$, is obtained by applying the very same process to the control group CONT.

3.2.4. Calculation of Mask Matrices

The existence of temporal correlation in a pair of regions of brain depends on the statistical relationship between the corresponding pair of signals. Therefore, the region pairs with high temporal correlations are expected to produce signal pairs with high mutual information value.

3.2.4.1. Quadrants. The locations of brain where 16 aptodes are placed as shown in Fig. 3.4. In this study, adjacent signals are grouped into *quadrants* as in Fig. 3.4 and Fig. 3.5. More precisely, the 4 quadrants are $\mathrm{Q}_1 = \{s_1, s_2, s_3, s_4\}$, $\mathrm{Q}_2 = \{s_5, s_6, s_7, s_8\}$, $\mathrm{Q}_3 = \{s_9, s_{10}, s_{11}, s_{12}\}$ and $\mathrm{Q}_4 = \{s_{13}, s_{14}, s_{15}, s_{16}\}$, which correspond to the left lateral prefrontal cortex, the left medial prefrontal cortex, the right medial prefrontal cortex and the right lateral prefrontal cortex, respectively.

Then, the mutual information $I(s_i, s_j)$ where $s_i \in Q_x$ and $s_j \in Q_y$ with $x, y \in \{1, 2, 3, 4\}$ can be masked by means of a 16×16 mask matrix defined as

$$[R_{xy}]_{ij} = \begin{cases} 1, & s_i \in Q_x, s_j \in Q_y \text{ and } i > j, \\ 0, & \text{otherwise.} \end{cases} \tag{3.7}$$

Note that R_{xy} is defined to be an upper triangular matrix with 0s at the diagonal. Since mutual information is symetric, that is $I(s_i, s_j) = I(s_j, s_i)$, analysis is limited to

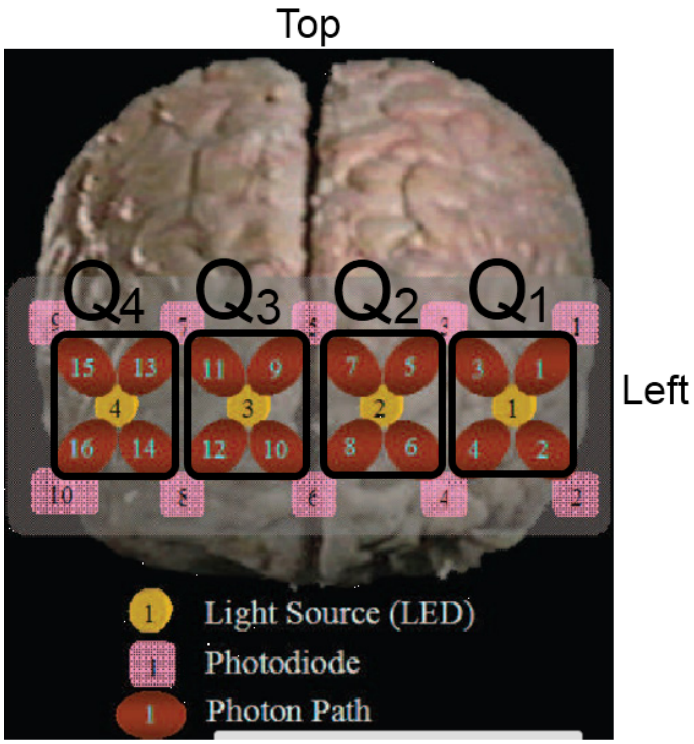

Figure 3.4. Placement of probes, source of signals and quadrants on the brain. Adopted from [41].

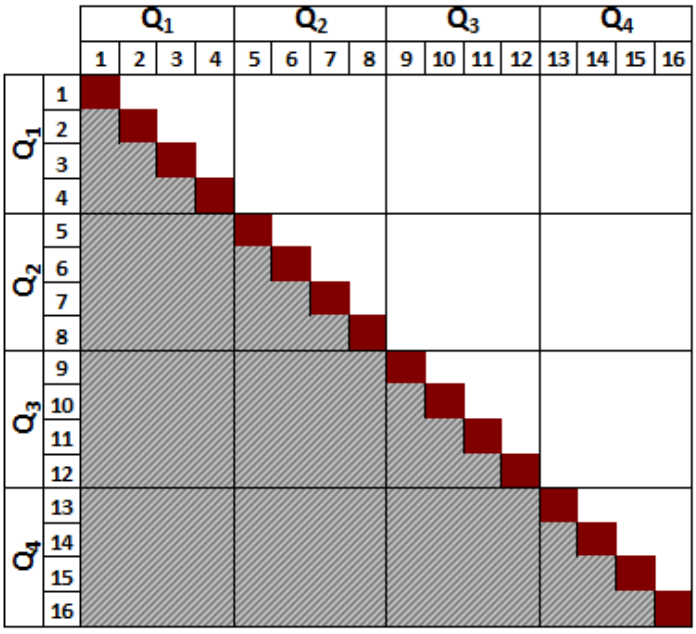

Figure 3.5. An 16×16 sample mask matrix. The lower triangle and the diagonal entries are all 0. Grouping of the signals into quadrants are also shown.

the upper triangular part of mutual information matrix. The mutual information of a signal with itself is, by definition, 1, therefore the diagonal entries do not carry meaningful information.

3.2.4.2. Selection of threshold. In the mutual information matrix, the high mutual information values imply high functional connectivity, where low mutual information imply low functional connectivity between the corresponding signal pairs. In order to focus on the high functional connectivity, the low mutual information values can be masked out by means of a proper mask matrix M. To do so, ξ-threshold operator with a proper ξ is applied. It can be easily noted that $0 \leqslant \xi \leqslant 1$ since $0 \leqslant I(i, j) \leqslant 1$.

The entries of the mutual information matrices, where the medication makes a statistically large difference, are essential and meant to provide reliable information which will be of use to identify mask matrix M. The "large" difference is iteratively identified by the thresold ξ.

Let's determine an acceptable upper limit for ξ. Given the sequences $\{A_k\}_{k=1}^{10}$ and $\{B_k\}_{k=1}^{10}$ of mutual information matrices, consider the difference of the averages

$$\Delta = \mu\left(\{B_k\}_{k=1}^{10}\right) - \mu\left(\{A_k\}_{k=1}^{10}\right). \tag{3.8}$$

which is also an 16×16 matrix. Then, on the average, the maximum effect of the medication in mutual information would be

$$\xi_0 = \max\left\{[\Delta]_{i,j}\right\} \quad \text{where} \quad i, j \in \{1, \ldots, 16\}. \tag{3.9}$$

Use ξ_0 as an upper bound for ξ.

Now a metric is needed to identify a proper ξ, where $0 \leqslant \xi \leqslant \xi_0$, which results high functional connectivity in the quadrants. The discriminative power of threshold

ξ, which is described below, is used as the metric to identify a proper ξ.

Let $t_{xy\xi}$ represent the score of t-test as a function of threshold ξ and quadrants pairs x-y. The algorithm used to calculate $t_{xy\xi}$ will be given shortly. A score, which is less than 0.05, is considered to be *statistically significant* while a score is said to be *statistically insignificant* if it is greater or equal to 0.05. For a given ξ, $t_{xy\xi}$ is calculated for all quadrant pairs x-y. As a result, some quadrant pairs have statistically significant and on the other hand some others have statistically insignificant $t_{xy\xi}$ scores. The *discriminative power of* ξ is the difference between the number of the statistically significant scores and the number of the statistically insignificant scores, for a given threshold ξ.

Table C.1 in Appendix C contains values of $t_{xy\xi}$ with respect to different x, y, ξ values. The rows correspond to the 10 quadrant pairs, along with the one which is the union of all masks. The columns correspond to the possible discrete values of threshold ξ in the range of $[0 - 0.16]$ with increments of 0.01. The upper bound is chosen as 0.16 since $\xi_0 = 0.1564$.

For a given threasold ξ, the significant values imply high functional connectivity while the insignificant values imply low functional connectivity in the corresponding quadrant pairs. Besides, the *N/A*s imply that none of the entries in the mutual information matrix that corresponds to the quandrant pairs x-y is greater than the threasold ξ, hence, t-test is not applicable. The *N/A*s may also be considered as information loss due to increase in ξ. So, there is a tradeoff between information loss and filtering quadrant pairs with high functional connectivity. Intuitively, to find an optimum solution for the trade-off, the lowest ξ value that meets the following two selection criteria, is chosen.

- Having the highest discriminative value
- Results no insignificant score.

In this point of view, the optimum value of ξ is found to be 0.08 in Table C.1.

Table C.2 in Appendix C is a refinement of the range [0.07−0.08] with increments of 0.001. Eventually, $\xi = 0.076$ is chosen, since it is the lowest ξ value that meets the selection criteria. In both tables, bold formatted cells represents the statistically significant values.

3.2.4.3. Calculation of $t_{xy\xi}$ values. Below is a step by step explanation of Fig. 3.6.

Input: The set of region pairs x, y such that $x \leqslant y \quad$ and $\quad x, y \in \{1, 2, 3, 4\}$ and the set of threasold ξ such that $0 < \xi < \xi_0$.

Output: The value of $t_{xy\xi}$ with respect to variables x,y and ξ.

begin
  foreach ξ *such that* $0 < \xi < \xi_0$ **do**
    $\tau_\xi \leftarrow \tau(\Delta, \xi)$
    $\beta_\xi \leftarrow \beta(\tau_\xi)$
    foreach x, y *pairs such that* $x \leqslant y \quad$ *and* $\quad x, y \in \{1, 2, 3, 4\}$ **do**
      $M_{xy\xi} \leftarrow \beta_\xi \odot R_{xy}$
      for $k = 1$ *to* 10 **do**
        $a_k \leftarrow \lambda\left(A_k, M_{xy\xi}\right)$
        $b_k \leftarrow \lambda\left(B_k, M_{xy\xi}\right)$
      end
      $t_{xy\xi} \leftarrow t\text{-test}\left(\{a_k\}_{k=1}^{10}, \{b_k\}_{k=1}^{10}\right)$
    end
  end
end

Figure 3.6. Calculation of $t_{xy\xi}$ values.

For each values of ξ,

(i) Apply ξ-threshold operation to obtain thresholded Δ matrix

$$\tau(\Delta, \xi) \tag{3.10}$$

(ii) Create a binary matrix from the threasolded matrix by replacing all values above zero.

$$\beta(\tau(\Delta, \xi)) \tag{3.11}$$

For each binary matrices calculated as a result of eq. (3.11)*, the following series of steps are performed*.

(iii) Consider the quadrants x and y. The binary matrix is masked by R_{xy} by appling $\odot$ operation to filter region of interest. Pick $M_{xy\xi}$ as a candidate binary mask matrix.

$$M_{xy\xi} = \beta\left(\tau\left(\Delta, \xi\right)\right) \odot R_{xy} \tag{3.12}$$

(iv) Apply average of non-zero entries operator λ using mask $M_{xy\xi}$ to the sequence of matrices to obtain a sequence of real numbers

$$\{a_k\}_{k=1}^{10} = \left\{\lambda\left(A_k, M_{xy\xi}\right)\right\}_{k=1}^{10} \text{ and } \{b_k\}_{k=1}^{10} = \left\{\lambda\left(B_k, M_{xy\xi}\right)\right\}_{k=1}^{10} \tag{3.13}$$

that are related to the region of interest R_{xy}.

(v) Apply t-test to $\{a_k\}_{k=1}^{10}$ and $\{b_k\}_{k=1}^{10}$ and then obtain $t_{xy\xi}$ which is a function of $x,\ y$ and ξ.

4. RESULTS AND DISCUSSION

A one-way ANOVA analysis was conducted among three groups of data, namely ADHD-OFF, ADHD-ON and CONTROL, to compare the effect of MPH on different prefrontal regions of brain.

Given the significance level of $\alpha = 0.05$, the result $F = 6.86, p = 0.0036$ in Table 4.1 indicates that the values of three groups differ significantly from each other. Moreover, the medians of three groups in Fig. 4.1 show that MPH increases the connectivity of prefrontal region of brain towards that of control group.

As to the pairs of quadrants, Q_2 - Q_3, Q_3 - Q_3 and Q_3 - Q_4 yielded significant difference with the results of $F = 7.59, p = 0.0022$; $F = 10.57, p = 0.0004$; $F = 5.15, p = 0.0122$ respectively. Also, the pairs of quadrants $Q_4 - Q_4$ showed marginal significant difference with the ratio $F = 3.11, p = 0.0598$. On the other hand, the comparison between the pairs of quadrants Q_1-Q_1 showed no significant difference with the F ratios $F = 1.04, p = 0.3674$. The list of ANOVA summary tables are grouped in Appendix A. The corresponding mask matrices and ANOVA notched box plots for the pairs of quadrants can be seen in Appendix B. Put in a nutshell, the ANOVA analysis revealed significant difference in mutual information between several brain regions.

In information theory, signal-to-noise ratio can be used as a metric to quantify *information rate*. In neuroscience, the neural network is considered to be a noisy

Table 4.1. ANOVA summary table for the union of all quadrants.

Source of Variation	**df**	**Mean Square**	**F**	**p**
Treatment	2	0.06891	6.86	0.0036
Error	29	0.1004		
Total	31			

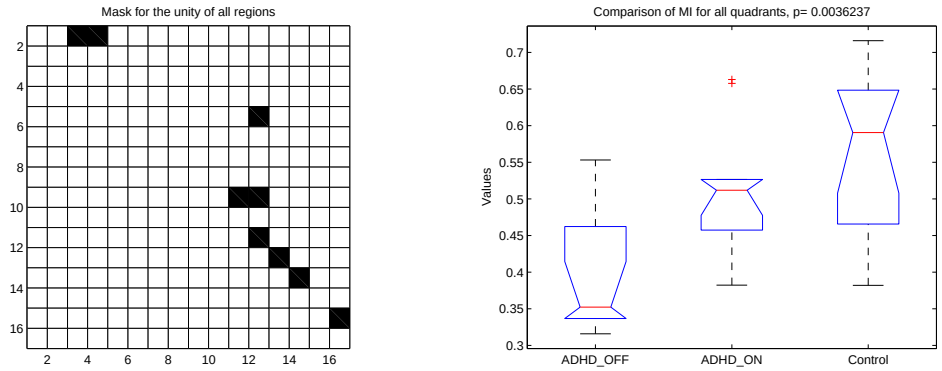

(a) The mask matrix

(b) ANOVA box plot

Figure 4.1. The mask matrix and the corresponding ANOVA box plot obtained by the ANOVA analysis applied to the union of all quadrants.

information source [65]. Hence, it can be concluded that the lower neural noise is, the higher the information that the signals carry. In this study, the information rate is evaluated by means of mutual information metric. The results revealed that right and left inferior prefrontal cortex (Q_1 and Q_4) in ADHD-OFF subjects exibits low mutual information values indicating higher noisy information flow. We came up with a conclusion that MPH medication lowers the noise level, thus, maximizes the signal-to-noise ratio and information flow. Our results are consistent with previous studies which suggests ADHD subjects have low signal-to-noise ratio [66,67].

It is said that the prefrontal cortex is one of the least well-understood region [68]. Attempts to effectively reveal the function of prefrontal cortex in functional neuroimaging have reported that right inferior prefrontal cortex mediates response inhibition and confliction detection [69,70]. In this study, the right inferior prefrontal cortex corresponds to the quadrant Q_4. So, the marginal significant difference among the signals in quadrant Q_4 shows that administration of MPH in ADHD subjects increases the ability of response inhibition and confliction detection in the right inferior prefrontal cortex. Hence, the mutual information among the signals in quadrants Q_4 seems to be an indirect indicator of ADHD.

Among the results, the significant difference between left and right medial prefrontal cortex (Q_2-Q_3) in Table A.2 and Fig. B.1b led us to an interesting conclusion. Since left and right medial prefrontal cortexes are located in different hemispheres, the information flow between these regions has to be carried over *the corpus callosum* which is a kind of bridge between the hemispheres. In many previous studies, the size of corpus callosum has been reported to have abnormalties in ADHD disordered individual [71–73]. Buchmann suggests that MPH may indirectly improve the function of callosal regions [74]. Our findings also support previous studies and show that administration of MPH may somehow improve the interhemispheric communication over the corpus callosum which is considered to be impaired in ADHD individuals. Yet more, we conclude that the improvement can be observed by the mutual information analysis on the temporal brain signals obtained from left and right medial prefrontal cortex (Q_2-Q_3).

The small number of ADHD subjects is the outstanding limitation of this study. In order to reduce the probability of Type I error, we have chosen a very low significance level $\alpha = 0.05$. Thus, the results are so significant that the Type I error is very unlikely.

Another important limitation of this study stems from the inability of fNIRS to penetrate the deep regions of the brain. Therefore, investigating relations between the frontal region and the internal region of the brain had to be out of the scope of the study. This kind of investigation is particularly needed to examine the connectivity between the prefrontal cortex and corpus callosum.

As a result, the information theoretical analysis lend enough credibility and evidence to the hypothesis that MPH normalizes ADHD subjects towards healthy controls.

5. CONCLUSIONS AND FUTURE WORK

Attention-deficit hyperactivity disorder is a common pediatric disorder persisting across adolescence and adulthood with characteristic symptoms of impulsivity, lack of attention and hyperactivity.

As one of the emerging brain imaging technologies, near infrared spectroscopy (NIRS) is used to detect and record brain signals that corresponds to hemodynamic changes in cerebral blood flow (CBF) during specific activities.

The aim of this study is to find out a statistical measurement model for mental diseases, particularly ADHD, by analysing brain signals with mutual information metric.

A group of 10 ADHD subjects (Age: 18-34, 4 females, 6 males) which were DSM-IV diagnosed formed the experimental group. On the other hand, a group of 12 age and gender matched healthy subjects were recruited to form the control group.

The subjects performed a revised version of the color-word matching Stroop interference test. During the Stroop test, subjects were presented a stack of two words. The upper word is ink colored, whereas the lower one is in solid black. The subject was supposed to detect and press left mouse button when the lower word is the color name of the upper word or press right mouse button otherwise. The meaning of upper word had no importance.

Mutual information analysis was carried out to quantify the information flow between regions of brain. Statistical analysis was performed to highlight the effect of medication on ADHD subjects. As expected, the medication made statistically significant difference on functional connectivity of brain regions. The results were finally compared by the previous studies and it is shown that the findings obtained

in this study overlap with those of previous studies.

As a result, the information theoretical analysis supported our hypothesis that MPH normalizes ADHD subjects towards healthy controls.

APPENDIX A: ANOVA SUMMARY TABLES

Table A.1. ANOVA summary table for Q_1-Q_1.

Source of Variation	df	Mean Square	f	p
Treatment	2	0.02762	1.04	0.3674
Error	29	0.02664		
Total	31			

Table A.2. ANOVA summary table for Q_2-Q_3.

Source of Variation	df	Mean Square	f	p
Treatment	2	0.0713	7.59	0.0022
Error	29	0.0094		
Total	31			

Table A.3. ANOVA summary table for Q_3-Q_3.

Source of Variation	df	Mean Square	f	p
Treatment	2	0.11734	10.57	0.0004
Error	29	0.0111		
Total	31			

Table A.4. ANOVA summary table for Q_3-Q_4.

Source of Variation	**df**	**Mean Square**	**f**	**p**
Treatment	2	0.07092	5.15	0.0122
Error	29	0.01377		
Total	31			

Table A.5. ANOVA summary table for Q_4-Q_4.

Source of Variation	**df**	**Mean Square**	**f**	**p**
Treatment	2	0.0797	3.11	0.0598
Error	29	0.02563		
Total	31			

APPENDIX B: ANOVA BOX PLOTS

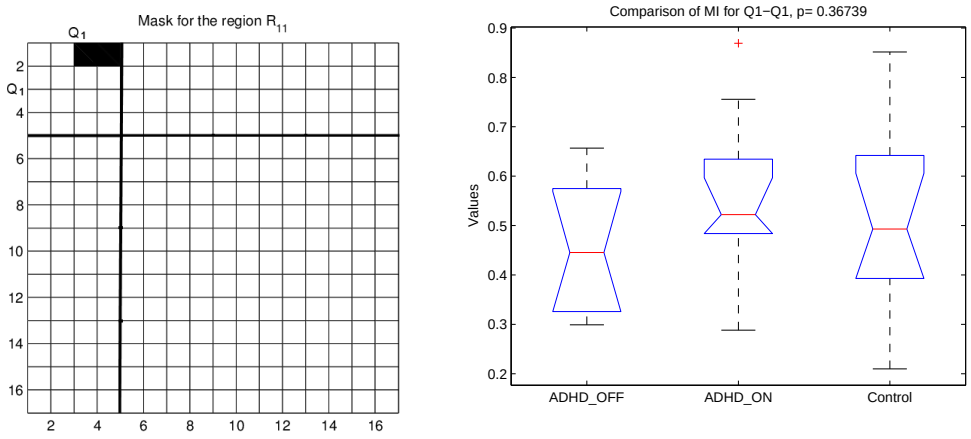

(a) Q_1 vs Q_1

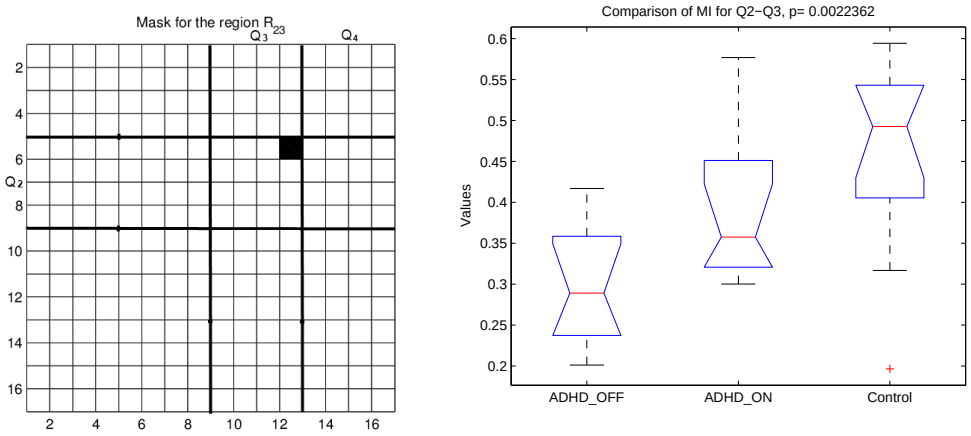

(b) Q_2 vs Q_3

Figure B.1. The mask matrices (Left) and the corresponding ANOVA box plots (Right).

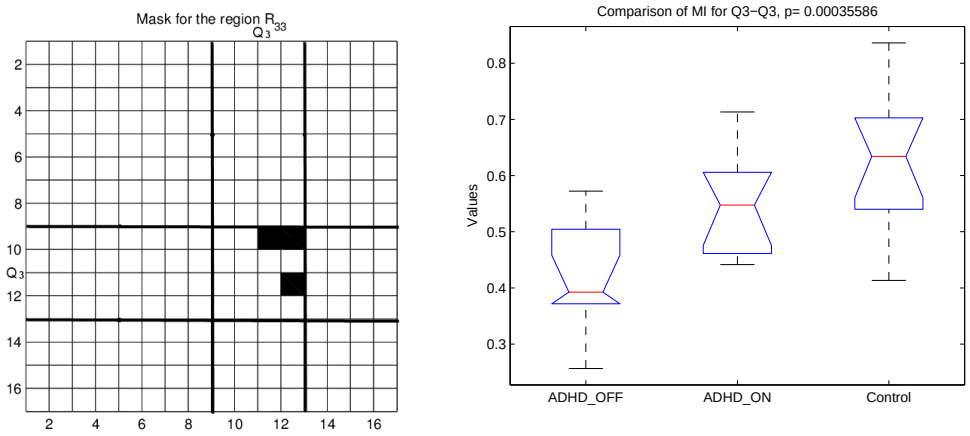

(c) Q_3 vs Q_3

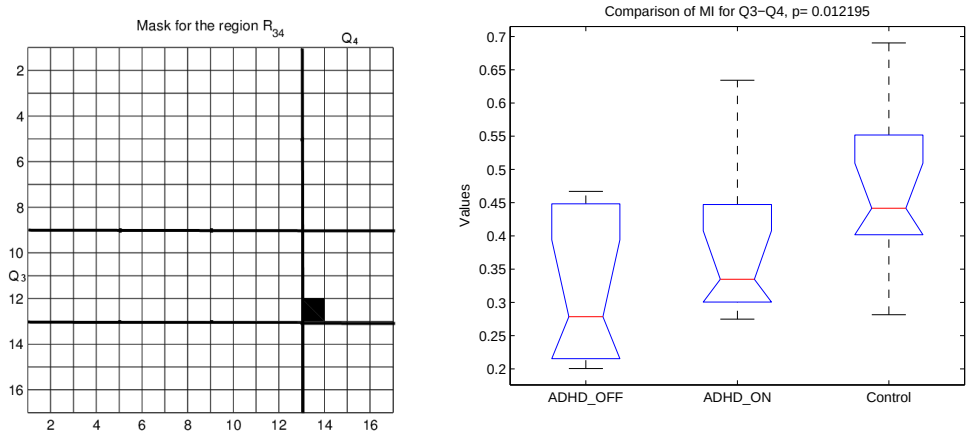

(d) Q_3 vs Q_4

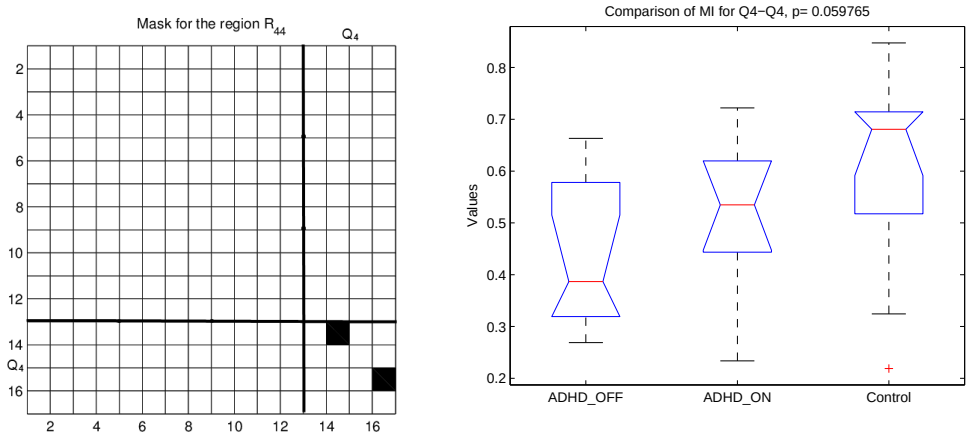

(e) Q_4 vs Q_4

Figure B.1. (Continued) The mask matrices (Left) and the corresponding ANOVA box plots (Right).

APPENDIX C: TABLE OF DISCRIMINATIVE POWER

Table C.1. Evaluation scores $t_{xy\xi}$ of discrete thresholds in the range [0 – 0.16]. Statistically significant values are in bold.

R_{xy} \ ξ	**0**	**0,01**	**0,02**	**0,03**	**0,04**	**0,05**	**0,06**	**0,07**	**0,08**	**0,09**	**0,10**	**0,11**	**0,12**	**0,13**	**0,14**	**0,15**	**0,16**
R_{11}	*0,058248*	*0,058248*	*0,058248*	*0,058248*	*0,058248*	*0,058248*	*0,058248*	***0,043592***	***0,043592***	***0,043592***	***0,046429***	***0,046429***	*N/A*	*N/A*	*N/A*	*N/A*	*N/A*
R_{12}	*0,495318*	*N/A*	*N/A*	*N/A*	*N/A*	*N/A*	*N/A*	*N/A*	*N/A*	*N/A*	*N/A*	*N/A*	*N/A*	*N/A*	*N/A*	*N/A*	*N/A*
R_{13}	*0,275858*	*0,262041*	*0,262041*	*0,243107*	*N/A*	*N/A*	*N/A*	*N/A*	*N/A*	*N/A*	*N/A*	*N/A*	*N/A*	*N/A*	*N/A*	*N/A*	*N/A*
R_{14}	*0,287667*	*0,219928*	*0,149384*	*0,149384*	*0,177155*	*N/A*	*N/A*	*N/A*	*N/A*	*N/A*	*N/A*	*N/A*	*N/A*	*N/A*	*N/A*	*N/A*	*N/A*
R_{22}	*0,181081*	*0,181081*	*0,151524*	*0,066856*	*0,066856*	*0,066856*	*0,066856*	*0,066856*	*N/A*	*N/A*	*N/A*	*N/A*	*N/A*	*N/A*	*N/A*	*N/A*	*N/A*
R_{23}	*0,123390*	*0,095305*	*0,095305*	*0,095305*	*0,056286*	***0,043034***	***0,031266***	***0,031266***	***0,031266***	***0,031266***	*N/A*	*N/A*	*N/A*	*N/A*	*N/A*	*N/A*	*N/A*
R_{24}	*0,253305*	*0,252485*	*0,242941*	*0,242941*	*N/A*	*N/A*	*N/A*	*N/A*	*N/A*	*N/A*	*N/A*	*N/A*	*N/A*	*N/A*	*N/A*	*N/A*	*N/A*
R_{33}	***0,001652***	***0,001652***	***0,001652***	***0,001652***	***0,001652***	***0,000498***	***0,000498***	***0,000063***	***0,000019***	***0,000019***	***0,000019***	***0,000031***	***0,000031***	***0,000031***	***0,000031***	***0,000031***	*N/A*
R_{34}	*0,126242*	*0,126242*	*0,070323*	*0,070323*	*0,062809*	***0,025434***	***0,025434***	***0,025434***	*N/A*	*N/A*	*N/A*	*N/A*	*N/A*	*N/A*	*N/A*	*N/A*	*N/A*
R_{44}	***0,032681***	***0,032681***	***0,032681***	***0,032681***	***0,032681***	***0,032681***	***0,025041***	***0,025041***	***0,044870***	***0,044870***	*N/A*	*N/A*	*N/A*	*N/A*	*N/A*	*N/A*	*N/A*
ALL	***0,035035***	***0,027141***	***0,016985***	***0,010926***	***0,004481***	***0,003164***	***0,004521***	***0,001607***	***0,000944***	***0,000944***	***0,000139***	***0,000825***	***0,000031***	***0,000031***	***0,000031***	***0,000031***	*N/A*
Number of significant scores	3	3	3	3	3	5	5	6	5	5	3	3	2	2	2	2	0
Number of insignificant scores	8	7	7	7	5	2	2	1	0	0	0	0	0	0	0	0	0
Discriminative power	-5	-4	-4	-4	-2	3	3	5	5	5	3	3	2	2	2	2	*N/A*

Table C.2. Refinement of the value range [0.07 − 0.08] in Table C.1. Bold cells in column of $\xi = 0,076$ are selected, since $\xi = 0,076$ is the lowest value having the largest discriminating power.

R_{xy} \ ξ	**0,070**	**0,071**	**0,072**	**0,073**	**0,074**	**0,075**	**0,076**	**0,077**	**0,078**	**0,079**	**0,080**
R_{11}	***0,043592***	***0,043592***	***0,043592***	***0,043592***	***0,043592***	***0,043592***	***0,043592***	***0,043592***	***0,043592***	***0,043592***	***0,043592***
R_{12}	*N/A*	*N/A*	*N/A*	*N/A*	*N/A*	*N/A*	*N/A*	*N/A*	*N/A*	*N/A*	*N/A*
R_{13}	*N/A*	*N/A*	*N/A*	*N/A*	*N/A*	*N/A*	*N/A*	*N/A*	*N/A*	*N/A*	*N/A*
R_{14}	*N/A*	*N/A*	*N/A*	*N/A*	*N/A*	*N/A*	*N/A*	*N/A*	*N/A*	*N/A*	*N/A*
R_{22}	*0,066856*	*0,066856*	*0,066856*	*0,066856*	*0,066856*	*0,066856*	*N/A*	*N/A*	*N/A*	*N/A*	*N/A*
R_{23}	***0,031266***	***0,031266***	***0,031266***	***0,031266***	***0,031266***	***0,031266***	***0,031266***	***0,031266***	***0,031266***	***0,031266***	***0,031266***
R_{24}	*N/A*	*N/A*	*N/A*	*N/A*	*N/A*	*N/A*	*N/A*	*N/A*	*N/A*	*N/A*	*N/A*
R_{33}	***0,000063***	***0,000063***	***0,000063***	***0,000063***	***0,000019***	***0,000019***	***0,000019***	***0,000019***	***0,000019***	***0,000019***	***0,000019***
R_{34}	***0,025434***	***0,025434***	***0,025434***	***0,025434***	***0,025434***	***0,025434***	***0,025434***	***0,025434***	***0,025434***	***0,025434***	*N/A*
R_{44}	***0,025041***	***0,025041***	***0,025041***	***0,025041***	***0,025041***	***0,025041***	***0,025041***	***0,025041***	***0,025041***	***0,044870***	***0,044870***
ALL	***0,001607***	***0,001607***	***0,001607***	***0,001607***	***0,002087***	***0,002087***	***0,000719***	***0,000719***	***0,000719***	***0,001081***	***0,000944***
Number of significant scores	6	6	6	6	6	6	6	6	6	6	5
Number of insignificant scores	1	1	1	1	1	1	0	0	0	0	0
Discriminative power	5	5	5	5	5	5	6	6	6	6	5

REFERENCES

1. Nass, R. D., "Evaluation and assessment issues in the diagnosis of attention deficit hyperactivity disorder.", *Seminars in pediatric neurology*, Vol. 12, No. 4, pp. 200–16, Dec. 2005.

2. Castellanos, F., J. Giedd, W. Marsh, S. Hamburger, A. Vaituzis, et al., "Quantitative brain magnetic resonance imaging in attention-deficit hyperactivity disorder.", *Arch Gen Psychiatry*, Vol. 53, No. 7, pp. 607–16, 1996.

3. McAlonan, G. M., V. Cheung, C. Cheung, S. E. Chua, D. G. M. Murphy, et al., "Mapping brain structure in attention deficit-hyperactivity disorder: a voxel-based MRI study of regional grey and white matter volume.", *Psychiatry research*, Vol. 154, No. 2, pp. 171–80, Feb. 2007.

4. Makris, N., S. L. Buka, J. Biederman, G. M. Papadimitriou, S. M. Hodge, et al., "Attention and executive systems abnormalities in adults with childhood ADHD: A DT-MRI study of connections.", *Cerebral cortex (New York, N.Y. : 1991)*, Vol. 18, No. 5, pp. 1210–20, May 2008.

5. Wolosin, S. M., M. E. Richardson, J. G. Hennessey, M. B. Denckla and S. H. Mostofsky, "Abnormal cerebral cortex structure in children with ADHD.", *Human brain mapping*, Vol. 30, No. 1, pp. 175–84, Jan. 2009.

6. Bush, G., E. M. Valera and L. J. Seidman, "Functional neuroimaging of attention-deficit/hyperactivity disorder: a review and suggested future directions.", *Biological psychiatry*, Vol. 57, No. 11, pp. 1273–84, Jun. 2005.

7. Schecklmann, M., A.-C. Ehlis, M. M. Plichta, J. Romanos, M. Heine, et al., "Diminished prefrontal oxygenation with normal and above-average verbal fluency performance in adult ADHD.", *Journal of psychiatric research*, Vol. 43, No. 2, pp. 98–106, Dec. 2008.

8. Herrmann, M. J., E. Woidich, T. Schreppel, P. Pauli and A. J. Fallgatter, "Brain activation for alertness measured with functional near infrared spectroscopy (fNIRS).", *Psychophysiology*, Vol. 45, No. 3, pp. 480–6, May 2008.

9. Ohta, H., B. Yamagata, H. Tomioka, T. Takahashi, M. Yano, et al., "Hypofrontality in panic disorder and major depressive disorder assessed by multi-channel near-infrared spectroscopy.", *Depression and anxiety*, Vol. 25, No. 12, pp. 1053–9, Jan. 2008.

10. Serap, S. and A. Akin, *Response inhibition in schizophrenia–an event-related fNIRS study*, IEEE, Apr. 2009.

11. Schecklmann, M., M. Romanos, F. Bretscher, M. M. Plichta, A. Warnke, et al., "Prefrontal oxygenation during working memory in ADHD.", *Journal of psychiatric research*, Vol. 44, No. 10, pp. 621–8, Jul. 2010.

12. Negoro, H., M. Sawada, J. Iida, T. Ota, S. Tanaka, et al., "Prefrontal dysfunction in attention-deficit/hyperactivity disorder as measured by near-infrared spectroscopy.", *Child psychiatry and human development*, Vol. 41, No. 2, pp. 193–203, Apr. 2010.

13. Schecklmann, M., E. Schenk, A. Maisch, S. Kreiker, C. Jacob, et al., "Altered frontal and temporal brain function during olfactory stimulation in adult attention-deficit/hyperactivity disorder.", *Neuropsychobiology*, Vol. 63, No. 2, pp. 66–76, Jan. 2011.

14. Salvador, R., J. Suckling, C. Schwarzbauer and E. Bullmore, "Undirected graphs of frequency-dependent functional connectivity in whole brain networks.", *Philosophical transactions of the Royal Society of London. Series B, Biological sciences*, Vol. 360, No. 1457, pp. 937–946, May 2005.

15. Bassett, D. S. and E. Bullmore, "Small-world brain networks.", *The Neuroscientist : a review journal bringing neurobiology, neurology and psychiatry*, Vol. 12, No. 6, pp.

512–23, Dec. 2006.

16. Lynall, M.-E., D. S. Bassett, R. Kerwin, P. J. McKenna, M. Kitzbichler, et al., "Functional Connectivity and Brain Networks in Schizophrenia.", *The Journal of neuroscience : the official journal of the Society for Neuroscience*, Vol. 30, No. 28, pp. 9477–9487, Jul. 2010.

17. Babiloni, F., F. Cincotti, C. Babiloni, F. Carducci, D. Mattia, et al., "Estimation of the cortical functional connectivity with the multimodal integration of high-resolution EEG and fMRI data by directed transfer function.", *NeuroImage*, Vol. 24, No. 1, pp. 118–31, Jan. 2005.

18. Salvador, R., A. Martínez, E. Pomarol-Clotet, S. Sarró, J. Suckling, et al., "Frequency based mutual information measures between clusters of brain regions in functional magnetic resonance imaging.", *NeuroImage*, Vol. 35, No. 1, pp. 83–8, Mar. 2007.

19. Barry Chai, Dirk Walther, Diane Beck and Li Fei-Fei, "Exploring Functional Connectivities of the Human Brain using Multivariate Information Analysis", Y. Bengio, D. Schuurmans, J. Lafferty, C. K. I. Williams and A. Culotta (Editors), *Advances in Neural Information Processing Systems*, Vol. 22, pp. 270–278, Advances in Neural Information Processing Systems, 2009.

20. Hlinka, J., M. Paluš, M. Vejmelka, D. Mantini and M. Corbetta, "Non-Gaussian dependence and neglected information in resting fMRI functional connectivity.", *NeuroImage*, Aug. 2010.

21. Getzfeld, A. R., *Essentials of abnormal psychology*, John Wiley & Sons, Inc, 2006.

22. Weiner, D. B., "Philippe Pinel's "Memoir on Madness" of December 11, 1794: a fundamental text of modern psychiatry", *American Psychiatric Association*, Vol. 149, pp. 725–732, 1992.

23. Pinel, P., *Traite medico-philosophique sur l'alienation mentale, ou La manie, 2nd Ed.*, Paris, Richard, Caille et Ravier, 1809.

24. Squire, L. R., J. L. Roberts, N. C. Spitzer, M. J. Zigmond, S. K. McConnell, et al., *Fundamental Neuroscience*, Academic Press, 2003.

25. Harlow, J. M., "Recovery from the passage of an iron bar through the head", *History of Psychiatry*, Vol. 4, No. 14, pp. 274–281, Jan. 1993.

26. Biederman, J., "Attention-deficit/hyperactivity disorder: a selective overview.", *Biological psychiatry*, Vol. 57, No. 11, pp. 1215–20, Jun. 2005.

27. Biederman, J. and S. V. Faraone, "Attention-deficit hyperactivity disorder.", *Lancet*, Vol. 366, No. 9481, pp. 237–48, 2005.

28. Friston, K. J., *Human Brain Mapping*, Wiley-Liss, Inc., 1994.

29. Frackowiak, R. S. J., K. J. Friston, C. D. Frith, R. J. Dolan, C. J. Price, et al., *Human Brain Function*, Academic Press, 2nd edn., 2003.

30. Purves, D., E. M. Brannon, R. Cabeza, S. A. Huettel, K. S. LaBar, et al., *Principles of cognitive neuroscience*, Sinauer Associates Inc., 2008.

31. Douw, L., M. de Groot, E. van Dellen, J. J. Heimans, H. E. Ronner, et al., "'Functional connectivity' is a sensitive predictor of epilepsy diagnosis after the first seizure.", *PloS one*, Vol. 5, No. 5, p. e10839, Jan. 2010.

32. Supekar, K., V. Menon, D. Rubin, M. Musen and M. D. Greicius, "Network analysis of intrinsic functional brain connectivity in Alzheimer's disease.", *PLoS computational biology*, Vol. 4, No. 6, p. e1000100, Jun. 2008.

33. Long, X.-Y., X.-N. Zuo, V. Kiviniemi, Y. Yang, Q.-H. Zou, et al., "Default mode network as revealed with multiple methods for resting-state functional MRI analysis.", *Journal of neuroscience methods*, Vol. 171, No. 2, pp. 349–55, Jun. 2008.

34. Wang, L., C. Zhu, Y. He, Y. Zang, Q. Cao, et al., "Altered small-world brain functional networks in children with attention-deficit/hyperactivity disorder.", *Human brain mapping*, Vol. 30, No. 2, pp. 638–49, Mar. 2009.

35. Liao, W., Z. Zhang, Z. Pan, D. Mantini, J. Ding, et al., "Altered functional connectivity and small-world in mesial temporal lobe epilepsy.", *PloS one*, Vol. 5, No. 1, p. e8525, Jan. 2010.

36. Bear, M. F., B. W. Connors and M. A. Paradiso, *Neuroscience: exploring the brain*, Lippincott Williams & Wilkins, 2007.

37. Akgül, C. B., *Analysis of Functional Near Infrared Spectroscopy Signals*, Master's Thesis, Bogazici University, 2004.

38. Serap, S., *Investigating Brain Hemodynamics of Schizophrenic Patients by Functional Near Infrared Spectroscopy*, Master's Thesis, Bogazici University, 2008.

39. Topaloğlu, N., *The Effect of Methylphenidate on Brain Hemodynamics of Attention-Decifit / Hyperactivity Disorder Measured by Functional Near Infrared Spectroscopy*, Master's Thesis, Bogazici Universtity, 2007.

40. Akin, A., D. Bilensoy, U. E. Emir, M. Gülsoy, S. Candansayar and H. Bolay, "Cerebrovascular dynamics in patients with migraine: near-infrared spectroscopy study.", *Neuroscience letters*, Vol. 400, No. 1-2, pp. 86–91, May 2006.

41. Aydöre, S., M. K. Mihçak, K. Ciftçi and A. Akin, "On temporal connectivity of PFC via Gauss-Markov modeling of fNIRS signals.", *IEEE transactions on bio-medical engineering*, Vol. 57, No. 3, pp. 761–8, Mar. 2010.

42. Çiftçi, K., B. Sankur, Y. P. Kahya and A. Akin, "Multilevel statistical inference from functional near-infrared spectroscopy data during stroop interference.", *IEEE transactions on bio-medical engineering*, Vol. 55, No. 9, pp. 2212–20, Sep. 2008.

43. Shannon, C. E. and W. Weaver, *The mathematical theory of communication*, Illini

Books, 1964.

44. Zhou, D., W. K. Thompson and G. Siegle, "MATLAB toolbox for functional connectivity.", *NeuroImage*, Vol. 47, No. 4, pp. 1590–607, Oct. 2009.

45. Wang, Z. J., P. W.-H. Lee and M. J. McKeown, "A novel segmentation, mutual information network framework for EEG analysis of motor tasks.", *Biomedical engineering online*, Vol. 8, No. 9, p. 9, Jan. 2009.

46. Brillinger, D. R. and A. Guha, "Mutual information in the frequency domain", *Journal of Statistical Planning and Inference*, Vol. 137, No. 3, pp. 1076–1084, 2007.

47. Gelfand, I.M. and Yaglom, A.M., "Calculation of the amount of information about a random function contained in another such function", *American Mathematical Society Translations, Series 2*, Vol. 12, p. 99, 1959.

48. Gosset, W. S., "The Probable Error of a Mean", *Biometrika*, Vol. 6, No. 1, pp. 1–25, 1908.

49. Gregersen, E. (Editor), *The Britannica Guide to Statistics and Probability*, Britannica Educational Publishing, 2011.

50. Peat, J. K. and B. Barton, *Medical statistics: a guide to data analysis and critical appraisal*, Blackwell Publishing, 2005.

51. Rossi, R. J., *Applied Biostatistics for the Health Sciences*, John Wiley & Sons, Inc, 2009.

52. Chernick, M. R. and R. H. Friis, *Introductory biostatistics for the health sciences: modern applications including bootstrap*, John Wiley & Sons, Inc, 2003.

53. Hulley, S. B., *Introductory biostatistics for the health sciences: modern applications including bootstrap*, Lippincott Williams & Wilkins, 2007.

54. Devore, J. L., *Probability and statistics for engineering and the sciences*, Thomson/Brooks/Cole, 2008.

55. APA, *Diagnostic and Statistical Manual of Mental Disorders, Fourth Edition, Text Revision (DSM-IV-TR)*, Vol. 1, American Psychiatric Association, Arlington, VA, 2000.

56. First, M. B., M. Gibbon, R. Spitzer and J. B. Williams, *Structured Clinical Interview for DSM-IV-TR Axis I Disorders, Research Version, Patient Edition With Psychotic Screen (SCID-I/P W/ PSY SCREEN)*, New York: Biometrics Research, New York: State Psychiatric Institute, 2002.

57. Stroop, J. R., "Studies of interference in serial verbal reactions.", *Journal of Experimental Psychology*, Vol. 18, No. 6, pp. 643–662, 1935.

58. Zysset, S., K. Müller, G. Lohmann and D. Y. von Cramon, "Color-word matching stroop task: separating interference and response conflict.", *NeuroImage*, Vol. 13, No. 1, pp. 29–36, Jan. 2001.

59. Perlstein, W. M., C. S. Carter, D. M. Barch and J. W. Baird, "The Stroop Task and Attention Deficits in Schizophrenia: A Critical Evaluation of Card and Single-Trial Stroop Methodologies", *Neuropsychology*, Vol. 12, No. 3, pp. 414–425, 1998.

60. MacLeod, C. M., "The Stroop Task: The "Gold Standard" of Attentional Measures", *Journal of Experimental Psychology*, Vol. 121, No. 1, pp. 12–14, 1992.

61. Roelofs, A., "Attention, temporal predictability, and the time course of context effects in naming performance.", *Acta psychologica*, Vol. 133, No. 2, pp. 146–53, Feb. 2010.

62. Çiftçi, R. K., *Statistical Analysis of Cognitive Signals Measured By fNIRS*, Ph.D. Thesis, Boğaziçi University, 2008.

63. Topaloğlu, N., E. Kara, E. Karahan, S. B. Erdoğan, S. Serap, et al., "The Effect

of Methylphenidate on Brain Hemodynamics of Attention-Deficit/Hyperactivity Disorder Measured by Functional Near Infrared Spectroscopy", *Biomedical Optics*, 2008.

64. Emir, U. E., *System characterization for a fast optical imager*, Master's Thesis, Bogazici University, 2003.

65. Borst, A. and F. E. Theunissen, "Information theory and neural coding.", *Nature neuroscience*, Vol. 2, No. 11, pp. 947–57, Nov. 1999.

66. Wolf, R. C., M. M. Plichta, F. Sambataro, A. J. Fallgatter, C. Jacob, et al., "Regional brain activation changes and abnormal functional connectivity of the ventrolateral prefrontal cortex during working memory processing in adults with attention-deficit/hyperactivity disorder.", *Human brain mapping*, Vol. 30, No. 7, pp. 2252–66, Jul. 2009.

67. Rubia, K., R. Halari, A. Cubillo, A.-M. Mohammad, M. Brammer, et al., "Methylphenidate normalises activation and functional connectivity deficits in attention and motivation networks in medication-naïve children with ADHD during a rewarded continuous performance task.", *Neuropharmacology*, Vol. 57, No. 7-8, pp. 640–52, Dec. 2009.

68. Ramnani, N. and A. M. Owen, "Anterior prefrontal cortex: insights into function from anatomy and neuroimaging.", *Nature reviews. Neuroscience*, Vol. 5, No. 3, pp. 184–94, Mar. 2004.

69. Rubia, K., A. B. Smith, M. J. Brammer and E. Taylor, "Right inferior prefrontal cortex mediates response inhibition while mesial prefrontal cortex is responsible for error detection.", *NeuroImage*, Vol. 20, No. 1, pp. 351–8, Sep. 2003.

70. Ridderinkhof, K. R., W. P. M. van den Wildenberg, S. J. Segalowitz and C. S. Carter, "Neurocognitive mechanisms of cognitive control: the role of prefrontal cortex in action selection, response inhibition, performance monitoring, and

reward-based learning.", *Brain and cognition*, Vol. 56, No. 2, pp. 129–40, Nov. 2004.

71. Semrud-Clikeman, M., P. A. Filipek, J. Biederman, R. Steingard, D. Kennedy, et al., "Attention-deficit hyperactivity disorder: magnetic resonance imaging morphometric analysis of the corpus callosum.", *Journal of the American Academy of Child and Adolescent Psychiatry*, Vol. 33, No. 6, pp. 875–81, 1994.

72. Schnoebelen, S., M. Semrud-Clikeman and S. R. Pliszka, "Corpus callosum anatomy in chronically treated and stimulant naïve ADHD.", *Journal of attention disorders*, Vol. 14, No. 3, pp. 256–66, Nov. 2010.

73. Cao, Q., L. Sun, G. Gong, Y. Lv, X. Cao, et al., "The macrostructural and microstructural abnormalities of corpus callosum in children with attention deficit/hyperactivity disorder: a combined morphometric and diffusion tensor MRI study.", *Brain research*, Vol. 1310, pp. 172–80, Jan. 2010.

74. Buchmann, J., W. Gierow, S. Weber, J. Hoeppner, T. Klauer, et al., "Modulation of transcallosally mediated motor inhibition in children with attention deficit hyperactivity disorder (ADHD) by medication with methylphenidate (MPH).", *Neuroscience letters*, Vol. 405, No. 1-2, pp. 14–8, Sep. 2006.